

AIP | Review of Scientific Instruments

Note: A simple-structured anode exchangeable X-ray tube

Thanh-hai Nguyen, Chang Jun Lee, Rae-jun Park, Gye-Hwan Jin, Sung Youb Kim et al.

Citation: *Rev. Sci. Instrum.* **84**, 056108 (2013); doi: 10.1063/1.4807755

View online: <http://dx.doi.org/10.1063/1.4807755>

View Table of Contents: <http://rsi.aip.org/resource/1/RSINAK/v84/i5>

Published by the AIP Publishing LLC.

Additional information on Rev. Sci. Instrum.

Journal Homepage: <http://rsi.aip.org>

Journal Information: http://rsi.aip.org/about/about_the_journal

Top downloads: http://rsi.aip.org/features/most_downloaded

Information for Authors: <http://rsi.aip.org/authors>

ADVERTISEMENT



physicstoday

Comment on any
Physics Today article.

Physics Today / Volume 63 / Issue 7 / July 2012
Previous Article | Next Article

Measured energy in Japan
David von Seggern
(dvs@seismo.unr.edu) University of Nevada
July 2012, page 10
DIGITAL OBJECT IDENTIFIER
<http://dx.doi.org/10.1063/PT.3.1619>
The article by Thorne Lay and Hiroo Kanamori (2012) is an excellent review of the relationship between seismic moment and energy release. However, they would find that the relationship between seismic moment and energy release is not linear. A 100-megaton nuclear explosion releases five times as much energy as a 20-megaton explosion, while that of a 300-megaton nuclear explosion releases approximately five times as much energy as a 60-megaton nuclear detonation event.

The 1964 Chilean earthquake had still more energy by a factor of about 3, or 15 times more energy than the 1964 nuclear device. I believe the authors used the relation for seismic energy release rather than total strain energy release. The seismic energy underestimates the total strain energy release by a variable that depends on the fault plane. Accounting for total strain energy release would increase the earthquake energy number by orders of magnitude.

Despite the catastrophic damage potential of nuclear bombs, the forces of nature occasionally unleash much larger energy releases. Although the nuclear bombs are under our control, earthquakes, volcanic eruptions, and extreme weather events are not. However, by judicious preparation and avoidance measures, humans can significantly diminish the damage of natural events.

This article does not have any references.

Comment on this article
By the act of hitting a ball with a bat, one calculates the force energy to deliver the ball to its new location, but one must also take into account that the ball extended its energy release to that location which became struck by the ball as its momentum ceased and passed energy to the struck team. Therefore the parameters of the damage extend into the future when the received energy to that pushed upon, later becomes released in a new event. Perhaps calculations of one added that in, while another's calculations did not. E.M.C.
Written by Edgar Mocarvill, 14 July 2012 19:59

Note: A simple-structured anode exchangeable X-ray tube

Thanh-hai Nguyen,¹ Chang Jun Lee,¹ Rae-jun Park,² Gye-Hwan Jin,³ Sung Youb Kim,⁴ and Insu Jeon^{1,a)}

¹*School of Mechanical Systems Engineering, Chonnam National University, 300 Yongbong-dong, Buk-gu, Gwangju 500-757, South Korea*

²*XL Co. Ltd., 1720-26 Taejang-dong, Wonju-si, Gwangwon-do 220-120, South Korea*

³*Department of Radiology, Nambu University, 76 Chumdan Jungang1-ro, Gwangsan-gu, Gwangju 506-706, South Korea*

⁴*School of Mechanical and Advanced Materials Engineering, Ulsan National Institute of Science and Technology, 100 Banyeon-ri, Eonyang-eup, Ulju-gun, Ulsan 689-798, South Korea*

(Received 15 March 2013; accepted 13 May 2013; published online 22 May 2013)

An anode exchangeable X-ray tube of very simple structure was developed. Aluminum, chromium, and copper anode targets were prepared and used to investigate X-ray spectra. X-ray images of a thin wood plate were taken using those targets. The measured energies of the characteristic X-rays of each target agreed well with the presented results. The difference of resolution and brightness of each image was found based on MTF values and intensities. The developed X-ray tube can give high durability, and higher quality X-ray images of an arbitrary object by exchanging anode targets. © 2013 AIP Publishing LLC. [<http://dx.doi.org/10.1063/1.4807755>]

Various types of X-ray tubes have been developed. Generally, the anodes of X-ray tubes were fabricated by using solid metals or liquid metals. X-ray tubes including solid metal anodes can be classified into the stationary anode type and rotating type. Stationary anode X-ray tubes are widely used, due to their simple design and low cost for fabrication. Electrons emitted from the filament cathode collide with the anode target surface and generate an X-ray spectrum.¹ However, less than 1% of those electrons produce X-rays, while the rest is converted into heat at the target surface. The temperature at the surface accumulates and rapidly increases under repeated electron collision. The high temperature damages the target surface and decreases the longevity of the X-ray tube. In order to solve this problem, a rotating anode target was developed, which increases the duration of the X-ray tube.² It can produce intense X-rays from the changed electron collision location on the rotating target. However, fabrication of the precise rotating device for anode target is complex and requires high cost.

Liquid metal anode targets for X-ray tubes were developed to overcome the drawbacks of solid metal anodes. The electron beam passes through the electron window of the tube and interacts with a liquid metal stream target flowing at high speed in a narrow channel in the tube.³ The liquid metal target plays the roles of X-ray generation medium and cooling medium. The demerits of the liquid metal anode X-ray tube were the lack of suitable kinds of liquid metal materials, and the complex structure of the tube and its additional system.

All the aforementioned X-ray tubes could generate only one kind of X-ray spectrum, dependent on the anode target material. Recently, an X-ray tube with multiple anode targets was developed to generate various characteristic X-rays.⁴ However, it has difficulties for installation of multiple targets in an X-ray tube, and for accurate mechanical adjustment of the target positions for keeping a constant focal spot size.

To improve the durability of X-ray tube and obtain various X-ray spectra, we developed a simple structure X-ray tube, for which the anode targets can be easily exchanged. Figure 1(a) shows a schematic drawing of the developed anode exchangeable X-ray tube. The comprehensive X-ray generator using the tube consists of a high voltage power supply, a vacuum pump system, and an internal water-cooling system. The anode target and filament cathode were installed inside the tube and connected with high voltage power supply. The pump system creates a vacuum state in the tube. In the system, the diffusion pump gradually decreases the normal pressure to the base pressure in the tube, while the turbo-molecular pump reduces the base pressure to the operational pressure in the tube at 5×10^{-7} Torr. The created vacuum state prevents burning out of the cathode, and arcing between the anode and cathode. A hollow structure was employed in the anode target, for direct internal-cooling. Water flow is circulated inside the target by an internal water-cooling system to increase the cooling rate up to $180 \text{ W/m}^2 \text{ K}$. In order to generate X-rays, the tungsten filament is first heated during a period of time by a heating circuit at 10 V and 5 mA. Then, electrons are emitted from the filament and hit the anode target surface to generate X-rays at high voltage. The X-rays pass through the low absorption thin Beryllium (Be) window and reach the object and detector.

The main frame of the tube is made of stainless steel and can be easily separated into two parts, by undoing bolts where the tungsten filament cathode is set in the upper part, and the hollow anode target is set in the lower part (see Figure 1(b)). The anode shoulder is positioned on the anode holder and fastened or unfastened by bolts for easy exchange, if the target is damaged during operation (see Figure 1(c)). For the experiments, aluminum (Al), chromium (Cr), and copper (Cu) anode targets were fabricated. Pure Al, Cu, and Cr materials were used for the targets. The size of the anode target was 22 mm in diameter and 30 mm in height. Its surface was tilted at an angle of 18° to the horizontal direction, to guide the

^{a)}E-mail: i_jeon@chonnam.ac.kr

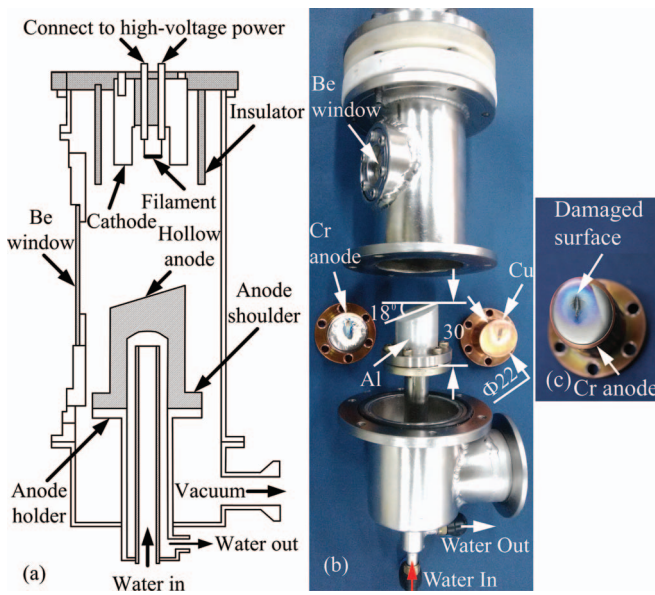


FIG. 1. (a) Schematic drawing of the anode exchangeable X-ray tube, (b) detached structure, and (c) damaged Cr target during long period of operation.

direction of X-rays. The size of the focal spot on the anode depends on the filament size and the angle of the inclined anode target surface. In this research, the focal spot size was designed at $2 \times 4.5 \text{ mm}^2$.

The X-ray spectra of Al, Cr, and Cu anode targets installed in the anode exchangeable X-ray tube were measured using an X-ray spectrometer with CdTe-diode, which has an allowable energy range from 5 keV to 150 keV (X-123CdTe, Amptek Inc.). The experimental setup to measure the X-ray spectra was shown in Figure 2(a). During experiments, a lead plate with a hole of $200 \mu\text{m}$ in diameter was set in front of the $100 \mu\text{m}$ thickness Be window of the spectrometer, to adjust the amount of photon flux. The distance from the X-ray tube to the spectrometer was fixed at 50 cm. The tube current was set at 0.5 mA, while the voltage was adjusted, depending on specific targets.

For measuring the X-ray spectrum of the Al anode target, an Al filter of $50 \mu\text{m}$ thickness was adopted to clearly detect the characteristic X-ray of the Al target after removing low energy level continuous X-rays. Considering the penetration of photons through the Al filter, it was set in front of the

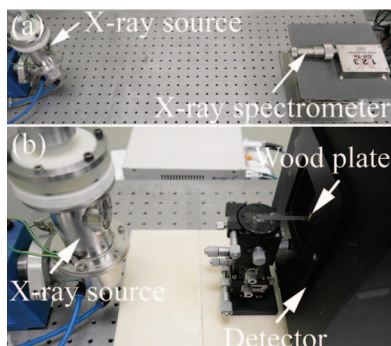


FIG. 2. Experiment set up for (a) measuring X-ray spectra, and (b) X-ray radiography.

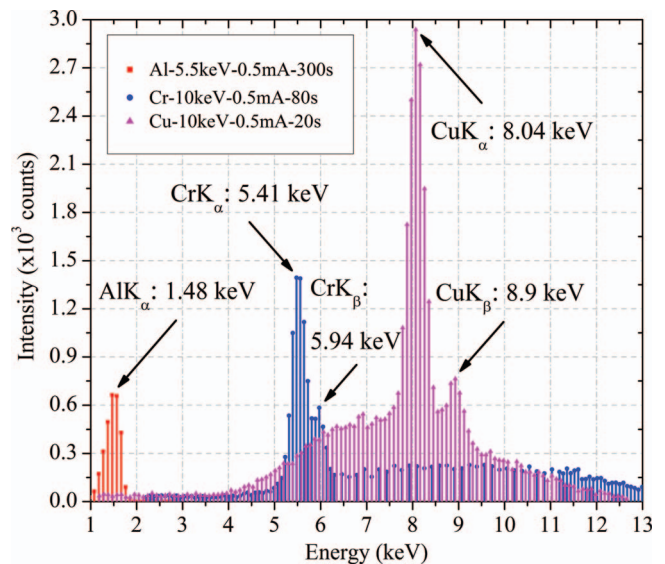


FIG. 3. Measured X-ray spectra of the Al, Cr, and Cu anode targets.

X-ray tube, and the X-ray exposing time was increased. Then, the X-ray spectrum was obtained at 5.5 keV, 0.5 mA, and 300 s. Relatively, lower electron voltage was applied than those for the Cr and Cu anode targets due to weakness of the Al target surface. The X-ray spectrum of the Cr anode target was obtained with a $10 \mu\text{m}$ thickness Al filter at 10 keV, 0.5 mA, and 80 s. The X-ray spectrum of the Cu anode target was obtained at 10 keV, 0.5 mA, and 20 s. The X-ray exposing time was decreased for the Cu target, because no Al filter was used for the measurement. All of the exposing times were decided for obtaining smooth X-ray spectra. The measured spectra of the Al, Cr, and Cu anode targets of the anode exchangeable X-ray tube are shown in Figure 3.

In Figure 3, the peaks of characteristic X-rays of each target are detected. In the case of the Cr anode target, the energy and intensity of characteristic X-rays CrK_α and CrK_β were found as 5.41 keV-1393 cps (count per second) and 5.94 keV-584 cps, respectively. The measured energies of characteristic X-rays agreed well with the results of Maeo *et al.*⁴ and Witte *et al.*⁵ The spectrum of the Cu anode target shows that the energy and intensity of characteristic X-rays CuK_α and CuK_β were 8.04 keV-2938 cps and 8.90 keV-763 cps, respectively. Their energies were also well matched with the results of Arkdiev *et al.*⁶ and Sato *et al.*⁷ The energy and intensity of characteristic X-ray of the Al anode target AlK_α were acquired as 1.48 keV and 664 cps, respectively. Those of AlK_β were not detected due to the weak intensity of AlK_β and the limited resolution of the spectrometer. However, it was found that the obtained energy of AlK_α agreed well with the result of Endo *et al.*⁸ From the results, we could confirm that the developed X-ray tube could give suitable X-ray spectra of various anode target materials.

Radiographies using the anode exchangeable X-ray tube were carried out (see Figure 2(b)). X-ray images were taken using each anode target. As an object, a thin wood plate of $5.2 \text{ mm} \times 2.29 \text{ mm} \times 0.6 \text{ mm}$ dimensions was prepared (see Figure 4(a)). The object was positioned at 200 mm from the source without filters and 3 mm before the scintillator, which

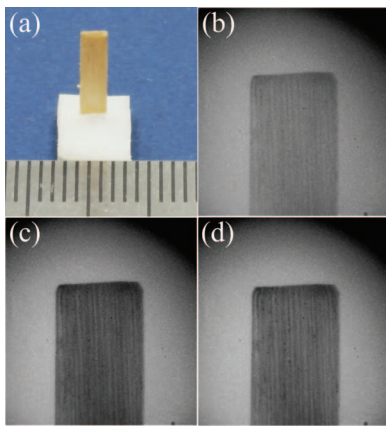


FIG. 4. (a) A wooden plate, and X-ray images taken using (b) Al, (c) Cr, and (d) Cu targets.

has CsI (Tl) columnar structures of $150\ \mu\text{m}$ thickness (ACS type, Hamamatsu, Japan), in a detector system. The detector system also contained a designed optical lens system with a magnifying power of 40.⁹ No slit or collimator for the tube was used to take X-ray images. The X-ray voltage, current, and exposing time were set at 20 keV, 10 mA, and 100 s for each anode target to compare the characteristics of obtained images with each other.

The obtained X-ray images of the wood plate using Al, Cr, and Cu anode targets are shown in Figures 4(b)–4(d). The fine structure of wood fibers was found in all the images. Hard fiber structures in the wood plate were seen as dark bands, and the soft tissues between those fibers were seen as bright bands. To compare the quality of each image, the modulus transfer function (MTF) values, which can be used to evaluate the spatial resolution of the obtained images, were calculated and plotted along the spatial frequency (see Figure 5(a)). The same region of interest at the upper-left edge of the wood plate in three X-ray images was selected for calculating the MTF values. Figure 5(a) shows that the MTF 50% of the X-ray images taken by Al, Cr, and Cu anode targets were 1.288, 1.417, and 1.672 lp/mm, respectively. This means the spatial resolution of X-ray image obtained from the Cu anode target is the best, and that obtained from the Cr anode target is the next, and that obtained from the Al anode target is the lowest. The higher spatial resolution gives better contrast and sharpness of X-ray images.

The intensity of each X-ray image, which was obtained from the summation of each pixel intensity along the vertical direction of each image, was calculated and plotted along

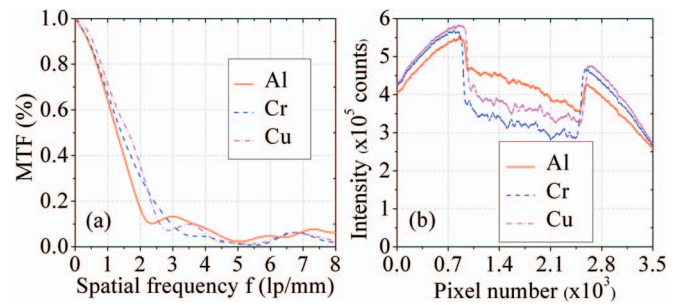


FIG. 5. (a) MTF changes along the spatial frequency, and (b) intensity changes along the pixel number.

pixel number in Figure 5(b). In the figure, it is found that the Al anode target gives the highest intensity, the Cu anode target gives the next, and the Cr anode target gives the lowest intensity. The higher intensity gives the higher brightness of X-ray images. The brightness change of X-ray images can also be confirmed in Figures 4(b)–4(d). It is considered that these difference of spatial resolution and intensity of each image stem from the different wavelengths of characteristic X-rays of each anode target material.

From the results, we see that the developed X-ray tube can be used for obtaining high quality X-ray images for an arbitrary object by selecting a suitable anode target material that generates specific characteristic X-rays. Also, it can provide a high durability with exchanging of anode targets, which were damaged during operation.

This work was supported by the National Research Foundation (NRF) of Korea grant, funded by the Korea government Ministry of Education, Science and Technology (MEST) (No. 2011-0031368).

¹C. S. Wong, S. Lee, C. X. Ong, and O. H. Chin, *Jpn. J. Appl. Phys.* **28**, 1264 (1989).

²E. A. Owen, *J. Sci. Instrum.* **30**, 393 (1953).

³B. R. David, H. Barschdorf, V. Doormann, R. Eckart, G. Harding, J.-P. Schlomka, A. Thran, P. Bachmann, and P. Flisikowski, *Proc. SPIE* **5196**, 432 (2004).

⁴S. Maeo, M. Kramer, and K. Taniguchi, *Rev. Sci. Instrum.* **80**, 033108 (2009).

⁵H. Witte, M. Silies, T. Haarlammer, J. Huve, J. Kutzner, and H. Zacharias, *Appl. Phys. B* **90**, 11 (2008).

⁶V. Arkadiev, H. Brauning, W. Burkert, A. Bzhaumikhov, H.-E. Gorny, N. Langhoff, A. Oppitz, and J. Rabe, *Nucl. Instrum. Meth. A* **455**, 589 (2000).

⁷E. Sato, Y. Hayasi, R. Germer, E. Tanaka, H. Mori, T. Kawai, T. Ichimaru, S. Sato, K. Takayama, and H. Ido, *J. Electron Spectrosc.* **137–140**, 705 (2004).

⁸S. Endo, M. Hoshi, J. Takada, T. Takatsuji, Y. Ejima, S. Saigusa, A. Tachibana, and M. Sasaki, *J. Radiat. Res.* **47**, 103 (2006).

⁹T.-H. Nguyen, S. Song, J.-H. Jung, and I. Jeon, *Opt. Lett.* **37**, 3777 (2012).